

Control of Capacitively Coupled Impedance source type Wireless Power Transfer Network

¹VadlakondaRanadeep, ²DoggaRaveendhra

^{1,2}Gokaraju Rangaraju Institute of Engineering and Technology, Bachupally, Hyderabad, India-500049

ABSTRACT: Capacitive power transfer (CPT), a wireless power transmission system based on electric field coupling, has been researched. A pair of "capacitors" in series with the power supply and load creates the CPT coupling interface. The effective capacitance is in the tens of hundreds of picofarads range, resulting in a high impedance. As a result, a tuning inductor is coupled in series with the coupling interface in most CPT systems for circuit compensation and improved power transfer capabilities. However, if the secondary side load is suddenly transferred, this compensatory mechanism suffers from strong voltage spikes from the inductor, posing electrical and health risks. This research presents a CPT system based on a Z-impedance compensation network that has intrinsic open-circuit and short-circuits immunity to address the problem. As a Z-source inverter, it also has the capacity to enhance voltage. Its working principle is discussed, as well as a set of design equations. On the secondary side, a (PI) controller is used to keep the charging current constant for the varying load. Additionally, a closed-loop circuit employing a PI controller was implemented for dynamic wireless electric car charging to prevent voltage variations caused by the varying spacing between both coils while the vehicle was in motion. It is then carried out to supply a constant voltage and constant current to the load. The control method's effectiveness is demonstrated through simulation results and a comparison with a single-level PI controller.

Index Terms— *Wireless power transfer, capacitive power transfer, compensation, Z impedance*

I. INTRODUCTION

Capacitive power transfer (CPT) technology, a recently suggested wireless power transfer technology, offers a new option for providing power to the load without galvanic connections via electric field coupling. CPT has a modest profile compared to inductive power transfer; low power losses, low electromagnetic interference, and the ability to transfer power over metal barriers as long as the coupling electric field is not entirely insulated are all advantages of this technology. It can be used to power low-power devices such as implanted biomedical devices and consumer gadgets.

CPT has also been used in high-power applications up to kilowatts, such as electric car charging. The structure of a typical CPT system is depicted in Figure 1. A capacitive coupling interface receives a high-frequency AC voltage generated by a power inverter from either a low-frequency AC or a DC power source. The coupling interface is made up of two pairs of conductive plates (such as aluminum or copper pads) that are insulated with dielectric materials. The plates' shape and size are determined by the application. Effective capacitances produced between plates are typically quite modest, ranging from a few tens to many hundreds of picofarads in most situations. Most CPT systems employ a single tuning inductor linked in series with the capacitive coupling to generate a series resonant tank to compensate for the large reactive impedance created by the capacitive coupling. The high voltage spikes created by the abrupt removal of the load make this approach prone to open-circuit faults, despite its simplicity and popularity. This is a common scenario for consumer electronics charging applications, where

the secondary coupling plates are used in conjunction with the primary coupling plates.

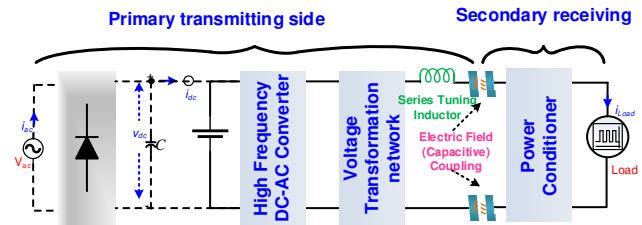


Fig. 1. Structure of a typical CPT system.

Although some CPT systems do not use series inductor compensation to supply a reasonable level of power, either relatively large coupling capacitances (tens of nanofarads) or extra sophisticated control circuitry for compensation is necessary. Without using a series tuning inductor, a CPT system based on a double-sided LLC topology is proposed; however, it necessitates additional reactive components on the secondary side, which increases size and cost, and the capacitor in parallel with the capacitive coupling interface must withstand high voltage stress. Furthermore, if the plates on the secondary side are damaged, the system is vulnerable to a short-circuit failure.

II. LITERATURE REVIEW

Because of health, comfort, & productivity, wireless electric vehicle charging has been widespread for a long time. A WPT network's effectiveness can be increased in a number of ways. Proposed Series-Series (SS) resonating remuneration geography close by the plan of radio recurrence criticism (Tan, 2017). This proposed model has undergone extensive testing. It was discovered that productivity about a 500W research facility model was greater than 90%, among an air hole about 15 cm, a distance of about 10 cm, & a working information voltage of about 120VAC (Tan, 2017). next technique considering improving WPT effectiveness to change working range from 81.38 to 90 kHz, (Ravikiran, 2017). The second approach used was to find a reference voltage in the optional side using concurrent assessment about the auxiliary side's common inductance & a voltage during the essential side (Hata, 2016). Furthermore, geographies play an important role in power move efficacy; thus, this article examines SS(series-series) & PS(parallel-series) showstopology in detail (Ravikiran, 2017). PS topology useful considering power usage about medium reach, according to reenactment results. To improve the transfer efficiency, this work uses optional side LCC impedance coordinating among circuits under a rectifier burden (Liao, 2017). It is critical to increasing the rate at which an electric car battery is remotely charged into stay informed about battery constraints.

One way to increase the battery execution to properly arrange the capacitor coupling variable & ensure that rate of discharge extremely fast (Klaus, 2017). It is using two additional loops in the middle about transmitter & collector coils among a 6.6KW circuit, another way to increase power transfer arrangement about an electric car (Tran, 2018). considering 3.4KW, this results in inefficiency of about 97.08 percent. This study recommended using a 20 enhanced floor surface considering guarding sending loop territory, high-recurrence

switches among large bandgap switches, & polygon iron centers to address various WPT issues (Mahmud, 2017). These sections contribute to the network efficiency. As a result, a distant power-involved charging network necessitates a constant current flow & a yield voltage that close to the highest productivity. This necessitates the creation of a control-based, most extreme productivity global positioning framework that regulates transmitter current based data received to Bluetooth near beneficiary (Yeo, 2017). This results in a constant voltage & a stable current stream among increased capacity in the WPT framework, effectiveness important. To improve the remote power charging network's efficiency, a fixed voltage source & fixed current load preserve displayed, evaluated, & checked provisionally (Zhang, 2017). distance between two loops determines voltage supplied in a wireless power transfer network. On the recipient side about wireless power transfer, this document executes a corresponding vital regulator Remove voltage variation considering a different distance between two plates (Yeo, 2017).

Furthermore, a strong electromagnetic field formed between transmitter loop & collector plates harmful to human health, necessitating the necessity to reducing attractive field spillage between loops. This level extremely high enormous air holes that occur between transmitter loop & recipient plate cause electromagnetic field spillage between two plates (Kim, 2016; Haque, 2018). One way via reducing attractive field spillage between two plates to design a framework among a low attractive spillage about approximately 19.8mG & a high WPT efficiency about around 80% 96 percent about way through a 156mm air hole (Zhang, 2016). To decrease network losses during turn on or off while EV traveling (Cho, 2016). An ideal accepted loop plan proportion about range 4, height 5, & distance 13, resulting in a half higher influence move efficiency.

Cho's research looked at the relationship between coupling coefficient & GPSSC's (Grouped Periodic Series Spiral Coupler Periodic Series Spir (Cho, 2016). Metamaterials, which help to focus attractive field, preserve another way to reducing electromagnetic field spillage between transmitter & recipient while simultaneously increasing power transfer productivity (Dolara, 2017). This research used a metamaterial to show that effectiveness was increased by around 44.2 percent & around 3.49dBm reduced appealing leakage at a distance of about more than 20 cm. Additionally, an appealing protecting approach employing conductive boards was presented via reduce danger associated with openness via an electromagnetic field about power cushion about an electric car (Campi, 2017), as well as an aluminum plate & ring (Campi, 2017). There were ideas considering lead emanation in charging electric vehicles remotely using SS & LCC topology shows in this work (Cho, 2016); results suggest that SS topology reduces WPT-directed emanations (Cui, 2018).

Because of the enormous power that passed through loops, they're a necessity to gather electromagnetic wellbeing requirements (Hui, 2013). According to findings, an individual sitting in or behind a car only marginally exposed to an electromagnetic field, therefore meeting electromagnetic wellbeing requirements. People in the vehicle preserve more vulnerable to an electromagnetic field (Mandip, 2011).

III. Z-Source Inverter

An impedance-source (or impedance-cared for) power converter (abbreviated as ZSC) presented to overcome obstructions & concerns about conventional source converters. The overall structure of ZSC is depicted in Figure 2. It makes use of a unique impedance organization (or circuit) via connecting voltage source converter & current source

converter primary circuits via secondary circuit considering providing new features not available in traditional voltage source & current source converters when a capacitor & inductor preserve used individually [10], a power source, load, or another converter can exist used. Figure-1. depicts a ZSC structure that uses a combination of switching devices such as IGBTs & diodes. Z-source concept applies to all dc-to-ac, ac-to-dc, & ac-to-ac converters, & dc-to-dc power change.

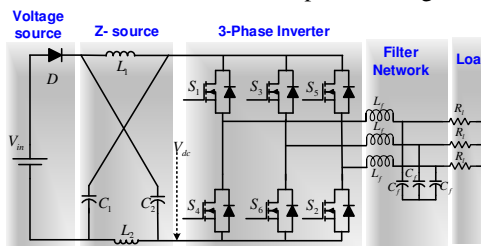


Figure 2: Structure of ZSI

The components that make up a ZSI's configuration preserve as follows:

1. Two Inductors
2. Two Capacitors
3. DC source
4. Inverter or Converter
5. Load or Converter

The ZSI's general structure is depicted in Figure-2. series combination of IGBT & diode is used in a ZSI construction. It overcomes old VSI & CSI's theoretical obstacles & restrictions, resulting in a novel power conversion approach. Figure 2 shows a two-port network among two split-inductors L_1, L_2 & capacitors C_1, C_2 connected in an X-direction Impedance source (Z-source) linking converter (or inverter) to dc supply, load, or another converter [10]. A voltage or current source/or load can exist used as source/or load. As a result, a battery, diode rectifier, thyristor converter, fuel cell, or inductor can all exist used as a dc source, a capacitor, or any combination about preceding. In the converter circuit, switches consist of a series of IGBTs & a diode. A split inductor or two different inductors can supply inductance L_1 & L_2 .

IV. Capacitive Power Transfer

Capacitive power transfer popularity considering powering & charging portable devices such as PDAs (personal digital assistant), cameras, & computers. The most often used setup nowadays involves an inductive [1,2] link between a charging station, which serves as a transmitter, & a collector, which frequently a handy device. When the transmitter is brought into proximity to the receiver, power flows from the transmitter to the receiver. Electrical plates preserve installed during both transmitter & receiver. We'll look at an alternative methodology that uses a capacitive rather than a resistive sensor.

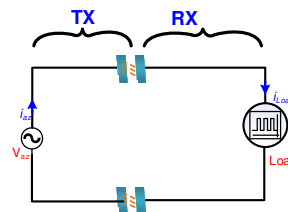


Figure 3: Power is transferred from an AC source to a load through capacitors formed by parallel plates on a transmitter and a receiver.

To deliver power than an inductive interface— Fig. 1. field restricted between conductive plates in a capacitive interface, considering requirement magnetic flux guiding & shielding components, which add bulk & cost to inductive

solutions [3]. amount about coupling capacitance that may exist achieved limited near device's available area, creating a difficult design constraint considering contactless devices delivery about power parallel plate capacitance across a 1/4 mm air gap, considering example, just 3.5 pF/cm², limiting average interface capacitance via a few tens about microfarads & requiring upwards about 2.5W about charging power (USB-specification). Existing capacitive power transfer (CPT) solutions either employ substantially bigger capacitors [4] or preserve designed considering lower-power applications, such as connection about two or more electrical devices Transmitting power&data via biosignal instrumentation systems [6,7] or between integrated circuits [5]. We put a lot of effort into circuit design & optimization via improving performance about presented results.

V. Circuit Description

The structure of the proposed CPT system among the Z impedance compensation network is shown in Figure 4 . A half-bridge inverter, a three-order LCC resonant tank, a Z impedance compensation network, a capacitive coupling interface made up of about two pairs of coupling plates,& a full-bridge rectifier followed near a DC load preserve all included.

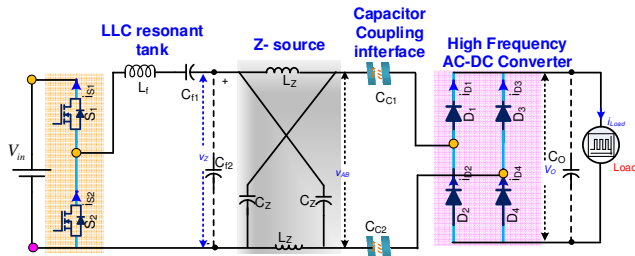


Fig. 4. Proposed CPT system with LCC and Z impedance compensation network.

A. LCC resonant network

Before Z impedance network, L_f , C_{f1} , & C_{f2} form an LCC resonant tank, & C_{f1} connected in series via block DC offset beginning voltage-fed half-bridge inverter (see Fig. 2). features about series & parallel LC tanks [20, 21] preserve combined in this LCC network to providing high efficiency at mild loading circumstances, which suitable considering CPT applications among loosely connected fluctuating loads. Other resonant tanks, such as series LC & LCL, can exist employed as well. On the other hand, a series LC tank does not have the ability to boost voltage, & an LCL tank requires an additional inductor, which increases the system's size & expense. Capacitor C_{f2} in parallel among Z impedance network serves via strength empower transfer capabilities about CPT systems near raising input voltage V_{IN} . LCC tank's components must satisfy the following equations:

$$C_{f1} = C_{f2} \tag{1}$$

$$C_f = \frac{C_{f1} * C_{f2}}{C_{f1} + C_{f2}} = \frac{C_{f2}}{2} \tag{2}$$

$$L_f = \frac{1}{\omega_s^2 C_f} = \frac{1}{\omega_s^2 C_{f2}} \tag{3}$$

where $\omega_s = 1/\sqrt{LC}$ is the operating frequency of the half-bridge inverter.

B. Z impedance compensation network

The Z impedance network has a symmetrical Z shape topology among two identical inductors L_z & two identical capacitors C_z . Z impedance network can enhance its input voltage V_z & compensate considering capacitive coupling interface, as discussed in the following sections. It's also resistant to open-circuit damage. Short-circuit failures preserve desired in CPT applications like powering portable consumer

devices. Because no inductor current stopped when load & secondary coupling plates preserve quickly transferred, no high voltage spikes preserve produced, which a significant improvement over the traditional compensating approach employing a single series inductor.

VI. Modeling of Z-Impedance Compensation

The steady-state properties of Z impedance compensation network preserve investigated using the sinusoidal approximation approach, assuming that converter in continuous conduction mode & that composite resonant tank has a strong Q response at excitation AC voltage's fundamental frequency. Characteristics of the Z impedance network can exist determined in the steady condition. A two-port network model can exist used to describe it. The voltage across parallel capacitor C_z has to be approximated as a sinusoidal AC voltage source V_z in Fig. 3. C_c capacitive coupling interface's effective capacitance $C_c = \frac{C_{c1} * C_{c2}}{C_{c1} + C_{c2}}$, & Rectifier's effective ac resistance among load, which equals $8R/2$ when a capacitive filter is used after the rectifier.

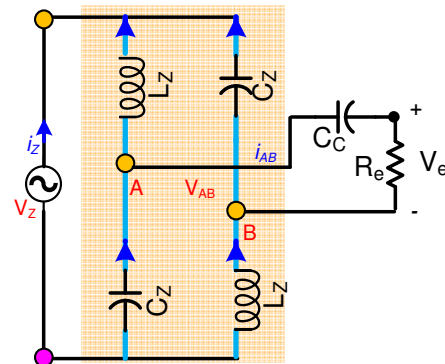


Fig. 5. The simplified circuit diagram of the CPT system with Z impedance network.

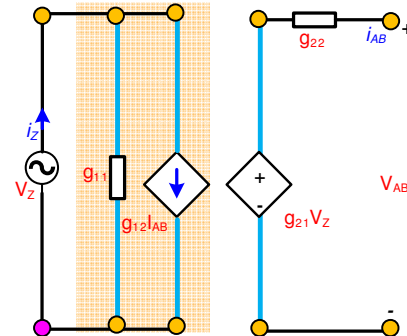


Fig. 6. The g-parameter description of the Z impedance network.

As illustrated in Fig. 4, the Z impedance network is modeled using g parameters. voltages & currents at terminals can exist described as follows,

$$\begin{aligned} I_z &= g_{11} V_z + g_{12} I_{AB} \\ V_{AB} &= g_{21} V_z - g_{22} I_{AB} \end{aligned} \tag{4}$$

The g parameters can exist calculated as shown in Fig. 3.

$$\begin{aligned} g_{11} &= \frac{I_z}{V_z} = \frac{2}{j\omega_s L_z + \frac{1}{j\omega_s C_z}} = \frac{2j\omega_s C_z}{1 - \omega_s^2 L_z C_z} \\ g_{12} &= g_{21} = \frac{V_{AB}}{V_z} = \frac{1 + \omega_s^2 L_z C_z}{1 - \omega_s^2 L_z C_z} \\ g_{22} &= \frac{V_{AB}}{I_{AB}} = \frac{2j\omega_s L_z}{1 - \omega_s^2 L_z C_z} \end{aligned} \tag{5}$$

Define Z impedance network's resonance frequency Z as

$$\omega_z = \frac{1}{\sqrt{L_z C_z}} \tag{6}$$

And normalized operating frequency about Z impedance network in relation via its resonant frequency can exist written as

$$F = \frac{\omega_s}{\omega_z} = \frac{\text{operating frequency}}{\text{resonant frequency}} \quad (7)$$

Substituting (6) and (7) into (5) yields

$$\begin{aligned} g_{11} &= j\omega_s C_z \frac{2}{1-F^2} \\ g_{12} &= g_{21} = \frac{1+F^2}{1-F^2} \\ g_{22} &= j\omega_s L_z \frac{2}{1-F^2} \end{aligned} \quad (8)$$

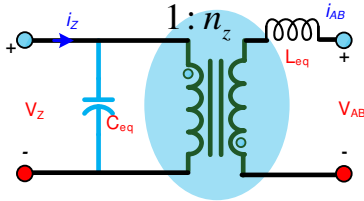


Fig. 7. The equivalent circuit model of the Z impedance network.

The g-parameter description can exist turned into an equivalent circuit model as shown in Fig. 5 near selecting suitable range about F. An ideal transformer among an effective turns ratio about n_z connects an input parallel capacitor C_{eq} via an output series inductor L_{eq} . Their values can exist derived directly beginning g parameters:

$$n_z = \frac{1+F^2}{1-F^2} \quad (9)$$

$$C_{eq} = \frac{2}{1-F^2} C_z \quad (10)$$

$$L_{eq} = \frac{2}{1-F^2} L_z \quad (11)$$

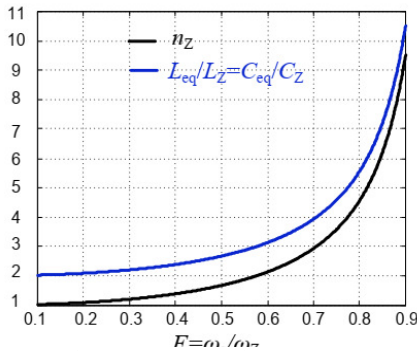


Fig. 8. Turns ratio n_z and normalized $L_{eq}/L_z(=C_{eq}/C_z)$ vs. F.

Because turns ratio about ideal transformer n_z always more than one when F less than one, Z impedance compensation network provides voltage boost capacity. Z impedance network's equivalent output inductance L_{eq} provides compensating functionality considering canceling capacitive coupling interface's impedance. It's worth noting that the input capacitance equivalent C_{eq} contributes via the LCC tank's parallel capacitor, which should be considered during the system design process. In Fig. 6, turns ratio n_z , as well as normalized values about L_{eq}/L_z & C_{eq}/C_z , preserve displayed against normalized frequency F. They all climb in lockstep among F, implying that a high voltage boost ratio N_z produced when F increased operating frequency close to Z impedance network's resonance frequency needed F_c via compensating coupling capacitance C_c considering a given value about L_z can exist computed beginning (11):

$$F_c = \sqrt{1 - 2\omega_s^2 C_z L_z} \quad (12)$$

which implies that $L_z < 1/(2\omega_s^2 C_c)$. Required C_z can exist obtained beginning definition about F

$$C_z = \frac{1 - 2\omega_s^2 C_c L_z}{\omega_s^2 L_z} \quad (13)$$

Therefore, the turns ratio n_z is

$$n_z = \frac{1 - \omega_s^2 C_c L_z}{\omega_s^2 C_c L_z} \quad (14)$$

In most cases, CC can exist treated as a fixed value considering a particular application. Fig. 7 shows variations about n_z & C_z/C_c among $L_z/(1/(\omega_s^2 C_c))$. It can be seen that smaller L_z yields a larger turns ratio n_z & C_z .

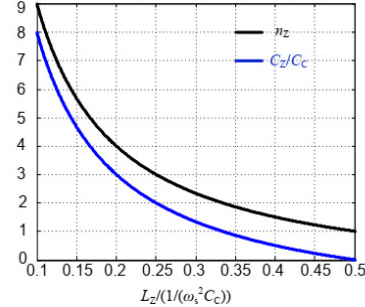


Fig. 9. The variations of turns ratio n_z and C_z/C_c versus $L_z/(1/(\omega_s^2 C_c))$

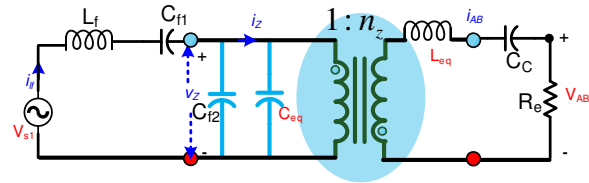


Fig. 10 Equivalent circuit of the proposed CPT system.

An equivalent circuit model about the system given in Fig. 8 using a derived circuit model about the Z impedance network. vs1 primary section about half-connect inverter's yield voltage. The same circuit can exist enhanced in Fig. 9 near referring to auxiliary side segments via essential side. Suppose identical yield inductance L_{eq} entirely compensates considering coupling, then among a larger equal capacitor ($C_{f2} + C_{eq}$) & a lower burden opposition (R_e/n_z^2). In that case, the proposed framework can exist reduced via an LCC resonant circuit. Following resolution about Z impedance network's bounds, real value about C_{f2} should consider C_{eq} , that is:

$$C_{f2,actual} = C_{f2,design} - C_{eq} \quad (15)$$

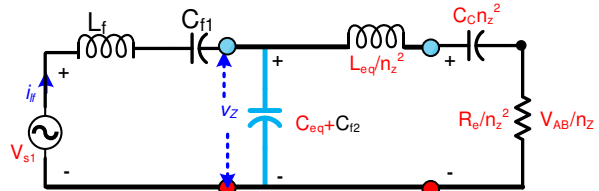


Fig. 11. The simplified circuit model of the proposed CPT system by reflecting components to the primary side through the ideal transformer.

In terms of L_z and C_c , C_{eq} can be expressed as

$$\frac{C_{eq}}{C_c} = \frac{1 - 2\omega_s^2 C_c L_z}{(\omega_s^2 C_c L_z)^2} \quad (16)$$

C_{eq}/C_c as a function about $L_z/(1/(\omega_s^2 C_c))$ illustrated in Fig. 10. It indicates that smaller L_z yields more significant equivalent input capacitance C_{eq} , tens about times larger than C_c if L_z is less than one-fifth about $1/(\omega_s^2 C_c)$.

Referring via Fig. 9, input impedance about resonant tank seen near input voltage vs1 can exist described as

$$\begin{aligned} Z_i &= \frac{1}{1 + Q_p^2 n_z^2} + j \left[\omega_s L_f - \frac{2 + \frac{1}{Q_p^2}}{\omega_s \left(1 + \frac{1}{Q_p^2}\right) C_{f2}} \right] \\ &= \frac{1}{1 + Q_p^2 n_z^2} + j \frac{1}{\omega_s C_{f2}} \frac{1}{1 + Q_p^2} \end{aligned} \quad (17)$$

$$Q_p = w_s C_{f2} \frac{R_e}{n_z^2} \tag{18}$$

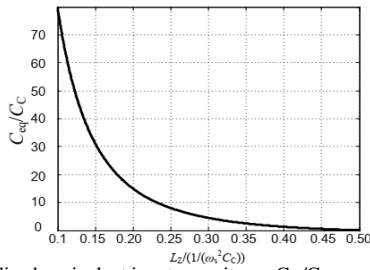


Fig. 12. Normalized equivalent input capacitance C_{eq}/C_c versus $L_z/(1/(\omega_s^2 C_c))$.

The inductive impedance governs time delay about zero crossing point about tank current produced near inductive impedance.

$$t_d = \frac{\arctan \frac{n_z^2}{w_s C_{f2} R_e}}{w_s} \tag{19}$$

The voltage $V_{Z,peak}$ value across the Z impedance network can exist written as

$$v_{z,peak} = \frac{v_{S1,peak}}{\|Z_i\|} \left\| \left(\frac{R_e}{n_z^2(1 + Q_p^2)} + \frac{Q_p^2}{jw_s(1 + Q_p^2)C_{f2}} \right) \right\| \tag{20}$$

$$= Q_p v_{S1,peak}$$

The output power PO can exist stated as follows, assuming 100% efficiency

$$P_o = \frac{2Q_p^2 n_z^2}{\pi^2 R_e} V_{IN}^2 \tag{21}$$

V_{IN} DC voltage input should exist noted that preceding equations preserve calculated using sinusoidal approximation method, implying that model's correctness determined near-resonant tank's quality factor. Primary objective about LCC tank via filter, which impactsthe performance about Z impedance compensation network. As a result, the LCC tank's characteristics must exist to ensure that quality factor Q_p is high. A trade-off must exist when deciding between a high voltage boost ratio n_z & a high-quality factor. WhileZ impedance compensation network has numerous advantages, such as open-circuit & short-circuit immunity, it also has certain disadvantages, such as a higher component count&a larger dimension. These issues can exist due to high operating frequency capacitor prices preserve low & current surface-mount technology used (SMT).

VII. Proportional and Integral Controller

The yield (also known as instigating signal) equal to total about relative & essential about error signal, as the name implies. Let's look at equivalent &essential regulators quantitatively right now. As we all know, yield about a corresponding & necessary regulator directly proportional via sum about relative about error & joining about blunder signal,& when we compose this numerically, we get,

$$A(t) \propto \int_0^t e(t)dt + A(t) \alpha e(t) \tag{22}$$

Removing the sign of proportionality, we have,

$$A(t) = K_i \int_0^t e(t)dt + K_p e(t) \tag{23}$$

Where K_i and k_p proportional constant and integral constant, respectively.

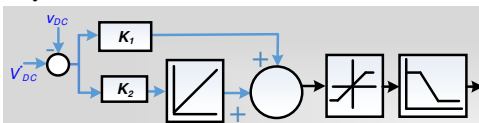


Fig13: Internal diagram of PI controller

The yield voltage about the proposed framework can exist modified near adjusting PI regulator reference esteem near using a PI regulator. Z-source network revealed a shared conviction between information & yield despite high voltage acquire &constant information current.

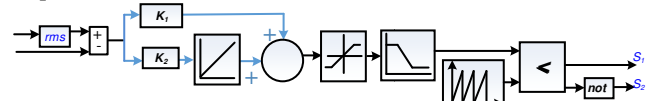


Fig14: Simulink model of PI controller

The voltage across necessary side plates & current through inductor L_f calmed down after a brief period when optional side plates were shorted, & no limit voltage or current spikes were formed during the transient period. Suggested Z-impedance remuneration system had little effect typical single arrangement inductor technique's high voltage spikes preserve limited.

VIII. Simulation Results

Figure 16 demonstrates that current into the LCC tank was less than the inverter's yield voltage, implying that the inverter achieved zero voltage exchanging (ZVS), resulting in lower exchanging misfortunes. Information voltage about Z impedance network in phase among current into it, as shown in Fig. 17, proves that the Z impedance network has entirely compensated considering the current interface about capacitive coupling.

Matlab Simulink used via demonstrating results about output voltages & currents, diode currents, inductor currents, & capacitor voltages considering a closed circle pi regulator based Z-source dc-dc converter. The waveforms about V_z & the optional side, which identical to V_z times n_z , preserve shown in Fig. 18. the voltage across AC resistive load is used to representing optional voltage because it a demonstrated voltage (they preserve equivalent when L_{eq} & C_c preserve at reverberation). It demonstrates that voltage v_z increased around 1.49 times.

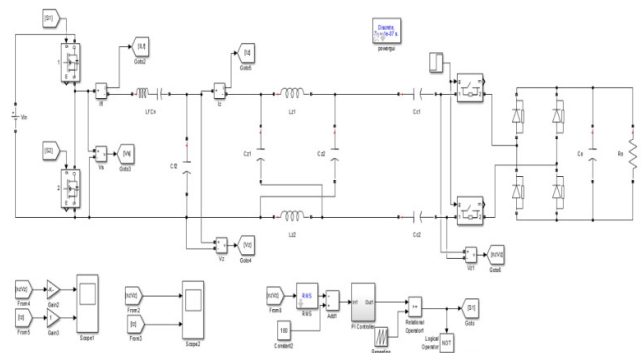


FIG 15. Simulink model of the proposed system

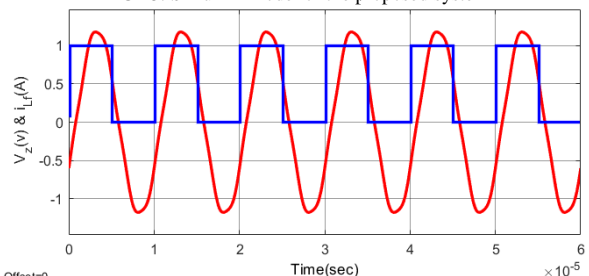


Fig. 16. Waveforms of the output voltage of the inverter and the current into the LCC tank

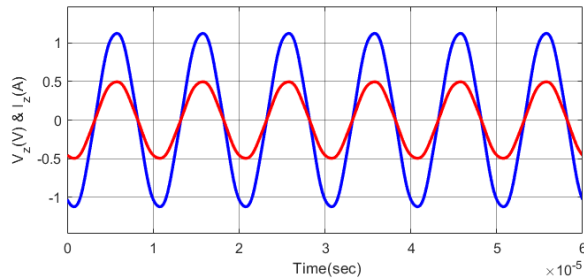


Fig. 17. Waveforms of the input voltage of Z impedance network and the current

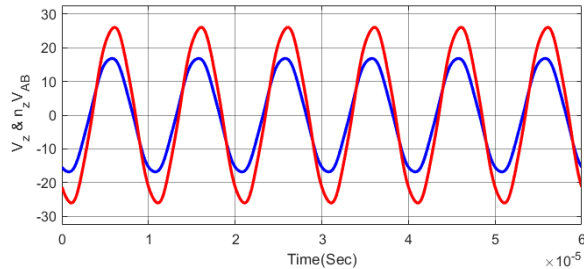


Fig. 18. Waveforms of the input voltage of Z impedance network v_z and the secondary side voltage.

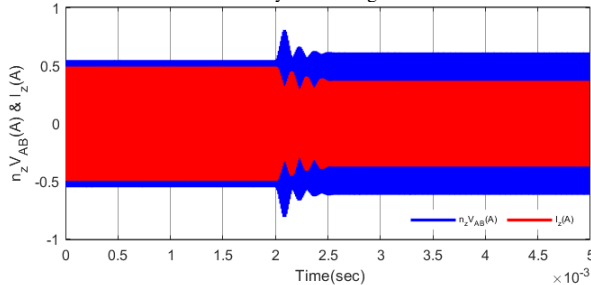


Fig. 19. Transient response of the voltage across the primary plates and the current through L_f after the sudden shorting of the secondary plates

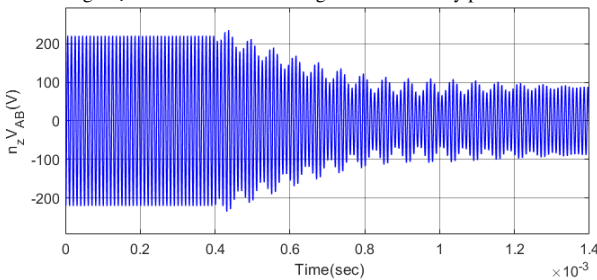


Fig. 20. Transient response of the voltage across the primary plates after the sudden removal of secondary plates of the CPT with the single series inductor compensation

IX. Conclusion

Customary single arrangement inductor shows strategy considering CPT networks experiences When auxiliary side plates preserve abruptly transferred, an open-circuit insufficiency occurs. Proposed Z impedance as follows can address this issue & give extra benefits, considering example, cut off & voltage support capacity. a shot circuit PI regulator was executed in this wireless power transfer network variety about voltage as a result about fluctuated dispersing existing between two plates, consequently, conveying a consistent to heap, apply a constant voltage & current. Among recreations & correlation among a single PI, adequacy about this control technique was validated.

X. References

[1]. A. P. Hu, L. Chao, and L. Hao Leo, "A Novel Contactless Battery Charging System for Soccer Playing Robot," in *Mechatronics and Machine Vision in Practice*, 2008. M2VIP 2008. 15th International Conference on, 2008, pp. 646-650.

[2]. L. Chao and A. P. Hu, "Steady state analysis of a capacitively coupled contactless power transfer system," in *Energy Conversion Congress and Exposition*, 2009. ECCE 2009. IEEE, 2009, pp. 3233-3238.

[3]. L. Chao, A. P. Hu, N. C. Nair, and G. A. Covic, "2-D alignment analysis of capacitively coupled contactless power transfer systems," in *Energy Conversion Congress and Exposition (ECCE)*, 2010 IEEE, 2010, pp. 652-657.

[4]. C. W. Van Neste, J. E. Hawk, A. Phani, J. A. J. Backs, R. Hull, T. Abraham, et al., "Single-contact transmission for the quasi-wireless delivery of power over large surfaces," *Wireless Power Transfer*, vol. 1, pp. 75-82, 2014.

[5]. L. Chao, A. P. Hu, and N. C. Nair, "Coupling study of a rotary Capacitive Power Transfer system," in *Industrial Technology*, 2009. ICIT 2009. IEEE International Conference on, 2009, pp. 1-6.

[6]. K. V. T. Piipponen, R. Sepponen, and P. Eskelinen, "A Biosignal Instrumentation System Using Capacitive Coupling for Power and Signal Isolation," *Biomedical Engineering*, IEEE Transactions on, vol. 54, pp. 1822-1828, 2007.

[7]. L. Huang, A. P. Hu, A. Swain, S. Kim, and Y. Ren, "An overview of capacitively coupled power transfer: A new contactless power transfer solution," in *Industrial Electronics and Applications (ICIEA)*, 2013 8th IEEE Conference on, 2013, pp. 461-465.

[8]. M. Kline, I. Izyumin, B. Boser, and S. Sanders, "A transformerless galvanically isolated switched capacitor LED driver," in *Applied Power Electronics Conference and Exposition (APEC)*, 2012 Twenty-Seventh Annual IEEE, 2012, pp. 2357-2360.

[9]. Murata Ltd. (2011, Dec 12). *Wireless power transmission modules* [Online]. Available: http://www.murata.com/products/wireless_power/index.html

[10]. J. Dai and D. C. Ludois, "Biologically inspired coupling pixilation for position independence in capacitive power transfer surfaces," in *Applied Power Electronics Conference and Exposition (APEC)*, 2015 IEEE, 2015, pp. 3276-3282.

[11]. F. Lu, Z. Hua, H. Hofmann, and C. Mi, "A Double-Sided LCLC Compensated Capacitive Power Transfer System for Electric Vehicle Charging," *Power Electronics*, IEEE Transactions on, vol. 30, pp. 6011-6014, 2015.

[12]. J. Dai and D. C. Ludois, "Wireless electric vehicle charging via capacitive power transfer through a conformal bumper," in *Applied Power Electronics Conference and Exposition (APEC)*, 2015 IEEE, 2015, pp. 3307-3313.

[13]. L. Chao, A. P. Hu, B. Wang, and N. C. Nair, "A Capacitively Coupled Contactless Matrix Charging Platform With Soft Switched Transformer Control," *Industrial Electronics*, IEEE Transactions on, vol. 60, pp. 249-260, 2013.

[14]. M. P. Theodoridis, "Effective Capacitive Power Transfer," *Power Electronics*, IEEE Transactions on, vol. 27, pp. 4906-4913, 2012.

[15]. L. Chao, A. P. Hu, G. A. Covic, and N. C. Nair, "Comparative Study of CCPT Systems With Two Different Inductor Tuning Positions," *Power Electronics*, IEEE Transactions on, vol. 27, pp. 294-306, 2012.

[16]. H. Fnato, Y. Chiku, and K. Harakawa, "Wireless power distribution with capacitive coupling excited by switched mode active negative capacitor," in *Electrical Machines and Systems (ICEMS)*, 2010 International Conference on, 2010, pp. 117-122.

[17]. D. Raveendhra and M. K. Pathak, "Three-Phase Capacitor Clamped Boost Inverter," in *IEEE Journal of Emerging and Selected Topics in Power Electronics*, vol. 7, no. 3, pp. 1999-2011, 2018, doi: 10.1109/JESTPE.2018.2873154, Print ISSN: 2168-6777, Electronic ISSN: 2168-6785 (Impact Factor: 5.177).

[18]. F. Z. Peng, "Z-source inverter," in *Industry Applications Conference*, 2002. 37th IAS Annual Meeting. Conference Record of the, 2002, pp. 775-781 vol.2.

[19]. N. Minh-Khai, J. Young-Gook, and L. Young-cheol, "Single-Phase AC-AC Converter Based on Quasi-Z-Source Topology," *Power Electronics*, IEEE Transactions on, vol. 25, pp. 2200-2210, 2010.

[20]. R. L. Steigerwald, "A comparison of half-bridge resonant converter topologies," *Power Electronics*, IEEE Transactions on, vol. 3, pp. 174-182, 1988.

[21]. M. K. Kazmierczuk, N. Thirunarayan, and S. Wang, "Analysis of series-parallel resonant converter," *Aerospace and Electronic Systems*, IEEE Transactions on, vol. 29, pp. 88-99, 1993.